ENGINEERING TRANSACTIONS • *Engng. Trans.* • **56**, 3, 247–268, 2008
Polish Academy of Sciences • Institute of Fundamental Technological Research

MODELLING OF THE ELECTROHYDRAULIC FULL ACTIVE VEHICLE SUSPENSION

J. K o n i e c z n y

Department of Process Control
AGH – University of Science and Technology
Kraków, Poland

The study investigates various models of vehicle suspensions. A quarter-vehicle full active suspension is chosen for further analysis. A mathematical model, governed by nonlinear differential equations, is proposed that takes into account dynamic properties of an electrohydraulic actuator. The mathematical model being implemented, it was expressed in terms of the state variables. In part two, the physical model was implemented and parametric identification procedure was applied. Phenomenological model simulation data are compared with results of experimental testing of a full, active vehicle suspension. The final section is focused on static and dynamic properties of an open-loop system (without a controller) determined on the basis of obtained models.

Key words: electrohydraulic actuator, full active, suspension, servovalve, model.

Notations

$\mathbf{A}$	state matrix,
$\mathbf{B}$	input matrix,
$\mathbf{B}_v$	input matrix corresponding to input v,
$\mathbf{B}_w$	input matrix corresponding to the excitation w,
$\mathbf{C}$	output matrix,
$\mathbf{D}$	feedforward matrix,
$\mathbf{I}$	identity matrix,
$\mathbf{x}$	state vector,
A_a	effective piston area; $A_a = 0.765786\ 10^{-3}$ m^2,
b_1	coefficient of viscous damping in the first DOF; $b_1 = 72$ Ns/m,
b_2	coefficient of viscous damping in the second DOF; $b_2 = 1161.2$ Ns/m,
C_d	flow discharge coefficient; $C_d = 0.611$ [–],
C_{tm}	leakage coefficient; $C_{tm} = 15 \cdot 10^{-12}$ m^5/Ns,
d	spool valve diameter; $d = 5 \cdot 10^{-3}$ m,
e	control error,
E	fluid bulk modulus; $E = 1.4 \cdot 10^9$ Pa,
f_{0i}	$i-$th natural frequency,
f_0	natural frequency,
F_l	leakage force,
F_p	force associated with flow,
f_s	actuator force,

F_{sc} fluid compressibility force,
h cylinder stroke; $h = 0.06$ m,
$\mathrm{Im}(\lambda)$ imaginary part of eigenvalue λ,
k_1 stiffness coefficient in the first DOF; $k_1 = 37412$ N/m (predicted value $k_1 = 44800$ N/m),
k_2 stiffness coefficient in the second DOF; $k_2 = 8652$ N/m (predicted value $k_2 = 8000$ N/m),
k_{sv} voltage to position conversion factor; $k_{sv} = 0.025 \cdot 10^{-3}$ m/V,
k_z stiffness coefficient of the suspension,
l spool valve perimeter; $l = 15,708 \cdot 10^{-3}$ m,
m_1 unsprung mass; $m_1 = 11.5$ kg,
m_2 sprung mass; $m_2 = 86$ kg,
P_d pressure in the lower chamber,
P_g pressure in the upper chamber,
P_r pressure difference,
P_z actuator supply pressure adjustable in the range 1–16 MPa; during the tests $P_z = 12$ MPa,
Q_l volumetric rate of leakage flow,
Q_z instantaneous flow rate between the unit and actuator,
R_1 flow cross-section; $R_1 = u_1 l$,
$\mathrm{Re}(\lambda)$ real part of eigenvalue λ,
u_1 spool displacement,
$u_{1\,\max}$ spool stroke; $u_{1\,\max} = 0.5 \cdot 10^{-3}$ m,
v servovalve control voltage,
V_p volume of hydraulic hose; $V_p = 80.0398 \cdot 10^{-6}$ m^3,
V_t total volume of actuator cylinder chambers; $V_t = 45.9458 \cdot 10^{-6}$ m^3,
w applied disturbance (displacement of an arbitrary contact point between suspension and road surface),
y output expressed in the space of state,
z displacement of the suspension in the vertical,
z_1 displacement of unsprung mass,
z_2 displacement of sprung mass,
α hydraulic coefficient; $\alpha = 44.4495$ N/m^5,
β_i angle between the i-th eigenvector and the real axis,
λ_i i-th eigenvalue of $\mathbf{A}$,
ρ fluid density; $\rho = 880$ Ns^2/m^4,
τ spool valve time constant; $\tau = 2.32 \cdot 10^{-3}$ s for $P_z = 12$ MPa,
ξ_i i-th damping ratio,
Φ nonlinear part of equation governing the actuator dynamics.

1. Introduction

Modelling of vehicle suspension is of key importance at the design stage. When active control systems are to be applied, the mathematical description allows the study of an open-loop system and helps in the synthesis of a control system. Accuracy of a mathematical model can be verified experimentally, by comparing the simulation and laboratory data. For that purpose, however, a physical model is required. This model is particularly useful whilst verifying the control algorithm for an actuator. This study refers to the synthesis and

verification of a mathematical model of an active suspension, with no control systems. Hence we consider an open-loop model, with no feedback. The model takes into account the properties of an electrohydraulic active actuator.

Vehicle suspension is a group of elements connecting the wheels with the rest of the vehicle, and is most difficult to design. Forces generated on the wheel-road surface interface are conveyed to the car body via the suspension. Its main function is to ensure the adequate comfort of the ride, vehicle stability and handling. The key elements include springs and dampers.

Springs enable the vertical movement of the suspension. The available spring types are: rubber springs, coil springs, leaf springs, pneumatic springs, gas-oil elastic elements, torsion bar. A vehicle equipped with springs only, is susceptible to oscillations when encountering an obstacle. When damping elements are used, the up and down movements of the vehicle are limited, depending on the oscillation velocity. Shock absorbers come in the form of oil-filled telescopic cylinders that resist sudden movements.

Suspension systems can be broadly classified into three subgroups: dependent, independent and semi-independent suspension systems. Passenger cars, where the ride comfort is a priority, are provided with independent suspensions only.

An interesting solution of an independent suspension in passenger cars is the McPherson strut-type suspension with simplicity of design as the major benefit. One sub-assembly operates during the ride, springing and damping of the road wheel vibration. A coil spring concentric with the shock absorber acts as an elastic element in this suspension.

There is a compact and separate unit for each wheel, hence an actuator can be employed instead of a shock absorber.

1.1. Suspension model analysis

In terms of physical representation, there are the following vehicle models with independent suspensions:

1) full 3D model,
2) half vehicle 2D model,
3) quarter vehicle 1D model.

In the full model the vehicle mass is represented by a lumped, sprung mass and four unsprung masses, each representing a wheel. Elements of the suspension placed between unsprung masses and the sprung mass are represented by springs and dampers, featuring reduced stiffness coefficient and viscous damping. Tires are modelled as springs with reduced stiffness ratio. Most tire models take into account the damping, J.A. Levitt [9] analyses the influence of a small

but nonzero relative damping term in the tire model ($\xi \approx 0.02$–0.05). Further damping reduces the vibration acceleration in the vertical direction by nearly 30%. The considered structure has 7 DOFs and enables the modelling of suspension's vertical displacement, pitch and roll of the vehicle body, and four vertical displacements of each of the wheels. Actually the model describes the behaviour of the system in all three planes. In active systems it is utilised to the synthesis of a master controller driving the whole suspension.

A half-vehicle model with 4 DOFs is frequently employed, too. The model takes into account longitudinal rolling, vertical displacements of the suspension and displacements in the vertical direction of the front and rear wheels. This model might also represent a half-suspension in the lateral direction, taking into account pitching, vertical displacements of the suspension and displacements in the vertical direction of the right and left wheel. No matter which plane, it will always be a 2D model with 4 DOFs. In the case of active suspensions controlling the vibrations of a vehicle represented by a quarter-car model, the synthesis of the controller should take into account the swaying effect (pitching or rolling).

A quarter-vehicle model featuring 2 DOFs is shown in Fig. 1.

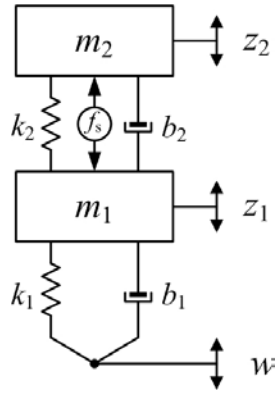

FIG. 1. Quarter-vehicle full active suspension.

Similarly to previous models, this model utilises the reduced stiffness coefficient of the suspension k_2 and the tire k_1 and the reduced viscous damping: of the suspension b_2 and the tire b_1. The mass m_2 is a reduced mass applying the load along one axis. It is a sprung mass and, as mentioned previously, the main function of the suspension is to maximally reduce its vibrations. The mass m_1 is called unsprung, representing chiefly the mass of a wheel and elements of the suspension. Variables z_2, z_1 and w stand for vertical displacements in the neighbourhood of the equilibrium point of the sprung and unsprung mass, and a given contact point between the tire and the road surface. This structure is

widely used in testing the control algorithms and actuators for the purpose of synthesis of active systems.

For clarity and comparability of research data, a quarter-vehicle model is chosen for further analyses. Besides, this structure enables the data verification in the existing laboratory setup. The model in Fig. 1 is provided with an actuator generating an active force f_s.

One can envisage several ways of placing an actuator in single-axis vibration isolation systems, yet the only structures to be employed in passenger cars with independent suspensions are full and slow active structures. Their major advantage is that they go on working (though in a limited degree) when an active system should fail. The main difference lies in that actuators in full active systems be designed such that their failure should not make them more rigid. In the case of slow active systems, an actuator failure should make it more rigid.

Full active suspensions, referred to as broadband or parallel structures, require an actuator operating in a wide frequency range (from 0 to 10–15 Hz). Broadband mode of the operation of the active system leads to major energy consumption. Its main advantage, on the other hand, is that no extensions of the suspension strut are required.

Slow active suspensions, known as narrow-band or limited-band, enables the actuator operation in the range of the first natural frequency of the suspension (from 0 to 3–4 Hz). It appears that this should reduce the external power demand in relation to parallel systems. The main drawback of suspension systems complete with an actuator mounted serially behind the spring is that the height of the suspension column has to be doubled. In order to retain the same stroke of the slow and full active suspensions, the stroke of the spring and actuator must be equal to the designed stroke of the suspension. Another disadvantage is that such suspensions are most sensitive to variations of the sprung mass, which might lead to unstable operation of the system when a spring is applied with a small stiffness coefficient. On account of low-frequency range of actuator operation, this structure is widely used to eliminate vibrations due to pitching (during braking or accelerating) and rolling (for example whilst cornering) [16].

That is why most active systems in vehicle suspensions have a parallel structure and this structure is analysed in this study. Physical implementation of such suspension consists in replacing a shock absorber by an actuator.

1.2. Actuators in vehicle suspensions

Electro-fluid actuators are widely employed as active force generators in concept of the active vehicle suspensions. In widespread use are hydraulic cylinders controlled by servovalves and electro-pneumatic elements utilising the compressibility of gas, which adds an extra elastic element to the system. Pneumatic

elements act as actuators in systems with ON/OFF controllers (rigid suspension – separated pneumatic chamber, soft suspension – added pneumatic chamber). Of particular interest are systems with linear electromagnetic motor. However, such actuators utilise permanent magnets and as it is necessary to generate sufficient force to lift the vehicle, their mass has to be very large. Another factor that precludes their widespread use is high cost associated with small-scale production of such elements.

This study explores electro-hydraulic actuators as they are most popular, at the same time satisfying the specified requirements in terms of force and stroke. Another reason why this particular actuator was selected is easy availability of the working medium in mechanical vehicles. The complete actuating system has a number of interacting hydraulic, electro-hydraulic and electronic assemblies. The main components include: a hydraulic feeder, a filtering unit, accumulator, servovalve, protecting and correcting elements, a hydraulic cylinder and control unit.

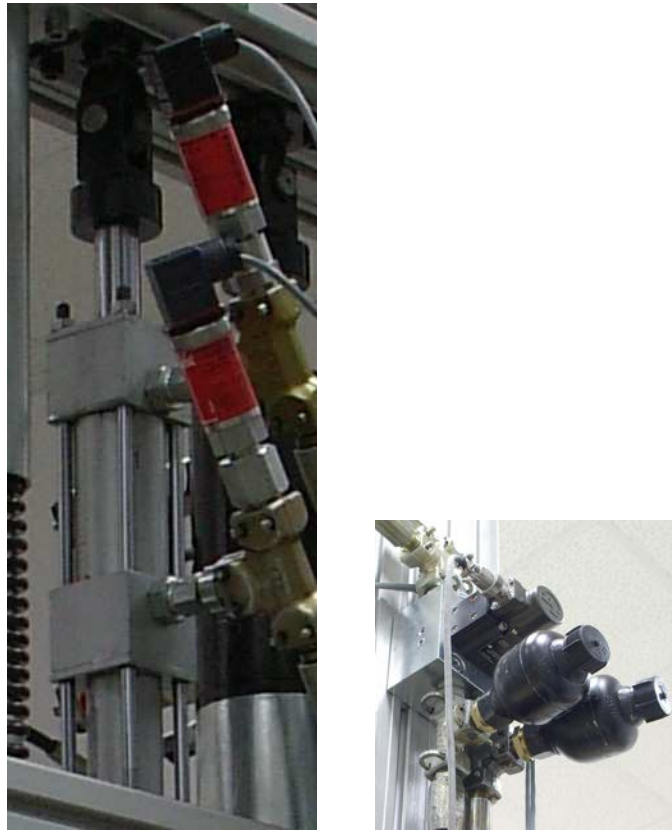

FIG. 2. Hydraulic cylinder with a control servovalve considered in the present study.

A servovalve is an electrohydraulic proportional divider controlling the hydraulic cylinder, it interacts with the control unit and, apart from the cylinder itself, becomes the key element that determines the dynamics of the whole electrohydraulic actuator assembly. A hydraulic cylinder with the servovalve considered in this study are shown in Fig. 2.

The measurement and control circuit comprising a number of transducers, a digital data processing unit, A/D and D/A modules and signal conditioning modules ought to ensure the adequate rate of signal processing and acquisition, if necessary.

The magnitude of force and displacements to be generated depends chiefly on geometric parameters of the hydraulic cylinder. The main function of the cylinder is to transmit mechanical energy to the suspension system in accordance with the selected control algorithm.

Protecting and correcting elements are of major importance too, as they prevent rapid pressure surges and associated hazards, which might lead to the system failure.

Dynamic properties of an active vibration reduction system depend not only on the actuators; the control system is another component that regulates the system dynamics (and hence the vibration isolation performance) and ensures a correct operation of the actuator.

2. Synthesis of a mathematical model

2.1. Mathematical model of an actuator

A hydraulic cylinder controlled by an electro-hydraulic servovalve is placed in parallel to the springs and a viscous damper, between the unsprung and sprung masses. It generates an active force f_s, whose main function is to minimise the displacement of the sprung mass m_2 with respect to an external reference system. The applied double-action cylinder with a two-sided rod is a special design. To minimise the resistance due to friction between its mobile elements, specially chosen sealing systems are applied in the rod and pilot sleeves. It is controlled by a double-stage four-way flow-control servovalve, 4WS2EM-type (601X/20 Rexroth). The servovalve is made in the standard version with mechanical feedback and zero overlap. Equations of actuator dynamics are derived on the basis of a diagram shown in Fig. 3.

Spool position control u_1 allows the liquid stream to be supplied from the source to one of the chambers in the cylinder and removed from the other chamber to the oil reservoir. The pressure difference P_r in chambers causes the working fluid to flow. Multiplying this pressure difference by the effective piston area A_a yields the actuator force f_s.

In order that the model should be expressed in the simplest terms at the same time retaining the vital properties of a real object, certain assumptions have to be made:

- the investigated system has lumped parameters,
- due to the presence of a large reservoir of the working fluid and the applied methodology, the effects of temperature on dynamic properties of an active system are neglected,
- temperature of the medium supplied to the system equals that of the medium inside the system,
- on account of the applied sealing strategy, the resistance force in a cylinder, associated with dry friction, is neglected,
- the flow in the system is turbulent, and continuity of the stream of working medium is maintained,
- conduits connecting the elements of the system are stiff and short and pressure loss of the flowing medium is negligible.

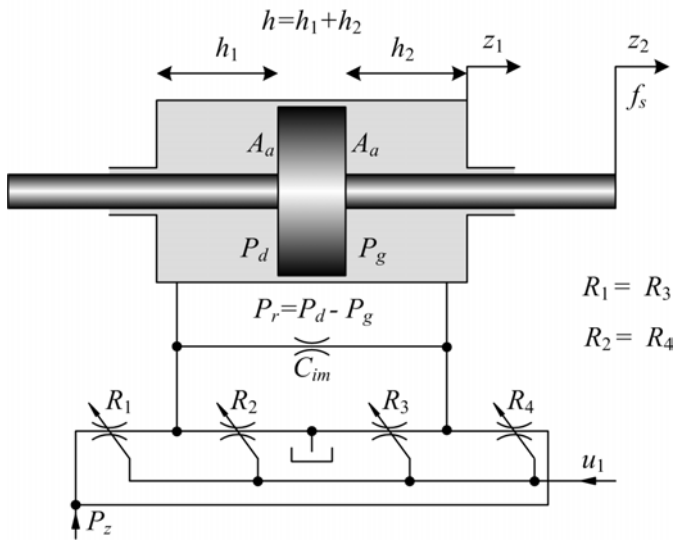

FIG. 3. Schematic diagram of active hydraulic element.

The dynamics of the system is written as an equation of force equilibrium

$$f_s = F_p - F_{sc} - F_l, \tag{2.1}$$

where: F_p – force associated with flow, F_{sc} – force of fluid compressibility, F_l – leakage force.

To derive the equation of state of a full active quarter-vehicle model complete with an actuator, the Eq. (2.1) is differentiated in the time domain yielding the derivatives of force components

$$\dot{f}_s = \dot{F}_p - \dot{F}_{sc} - \dot{F}_l \,. \tag{2.2}$$

Force of compressibility is obtained directly from the following equation [11]:

$$\frac{F_{sc}}{z_2 - z_1} = \frac{4EA_a^2}{V_t + V_p} \tag{2.3}$$

where: $z_2 - z_1$ – piston displacement relative to the cylinder, E – fluid bulk modulus, V_t – total volume of actuator cylinder chambers, V_p – volume of hydraulic hose.

A coefficient $\alpha = \dfrac{4E}{V_t + V_p}$ is used to describe hydraulic parameters. Accordingly, we get

$$\frac{F_{sc}}{z_2 - z_1} = \alpha A_a^2 \,. \tag{2.4}$$

Differentiating Eq. (2.4) with respect to time yields a formula expressing the derivative of the fluid compressibility force

$$\dot{F}_{sc} = \alpha A_a^2 \left(\dot{z}_2 - \dot{z}_1\right). \tag{2.5}$$

The equation of flow is written as

$$A_a \left(\dot{z}_2 - \dot{z}_1\right) = Q_l \,, \tag{2.6}$$

where Q_l – volumetric flow, governed by the formula

$$Q_l = C_{tm} P_r \,, \tag{2.7}$$

where C_{tm} – leakage coefficient.

Directly from Eq. (2.6) and using Eq. (2.5) and (2.7), we get

$$\dot{F}_l = \alpha A_a C_{tm} P_r \,. \tag{2.8}$$

The equation of flow between a symmetrical cylinder and a four-way servovalve is given by formula (2.9) [15]

$$A_a \left(\dot{z}_2 - \dot{z}_1\right) = R_1 C_d \sqrt{\frac{P_z - \operatorname{sign}\left(u_1\right) P_r}{\rho}} \,, \tag{2.9}$$

where: u_1 – spool displacement, R_1 – flow cross-section, $R_1 = u_1 l$ (l – spool circumference equal πd, d – spool valve diameter), C_d – flow discharge coefficient, for turbulent flow $C_d = \pi/\pi + 2 = 0.611$, P_z – supply pressure, ρ – fluid density.

Multiplying both sides of Eq. (2.9) by the derivative of force F_p and making use of Eq. (2.5), we get

$$\dot{F}_p = u_1 l \alpha A_a C_d \sqrt{\frac{P_z - \text{sign}\,(u_1)\, P_r}{\rho}}\,. \tag{2.10}$$

Substituting Eqs. (2.5), (2.8), (2.10) into Eq. (2.2) expressing the derivative of the control force, yields

$$\dot{f}_s = u_1 l \alpha A_a C_d \sqrt{\frac{P_z - \text{sign}\,(u_1)\, P_r}{\rho}} - \alpha A_a^2 \left(\dot{z}_2 - \dot{z}_1\right) - \alpha A_a C_{tm} P_r\,. \tag{2.11}$$

Quantities u_1, P_r, $\dot{z}_2$ $\dot{z}_1$ are time-dependent, other coefficients have constant values given in the Nomenclature section.

A relationship is also provided between the control force and the pressure difference, expressed by the formula

$$f_s = P_r A_a\,. \tag{2.12}$$

Spool position u_1 is controlled by the current level in coils of the servovalve motor. Hence, the spool dynamics can be approximated by a differential equation of the first order

$$\tau \dot{u}_1 + u_1 = k_{sv} v\,, \tag{2.13}$$

where: τ – time constant of the servovalve, k_{sv} – voltage-to-position conversion factor, v – servovalve control voltage.

This approximation appears to be sufficiently accurate for frequencies up to 50 Hz [3, 7, 14].

Equations (2.11)–(2.13) underlie the mathematical model of a vehicle suspension, complete with a electro-hydraulic actuator shown in the space of state.

2.2. Quarter-car model

Figure 1 shows a parallel quarter-car model of a vehicle, with lumped parameters. This is a 2 DOF model. The first DOF associated with mass m_1 applies to the part representing the wheel and tire. The mass of the wheel is unsprung. The second DOF – associated with the mass m_2 – applies to the car body mass with passengers. This mass is referred to as sprung. The main function of the analysed system is to minimise the vibrations of the mass m_2, is spite of disturbances caused by road roughness.

The model uses the following designations:
v – input – servovalve control voltage, which directly controls force f_s,
w – input – can be treated as disturbance due to road irregularities,
z_2 – displacement of the sprung mass.

Equations of motion of the unsprung mass m_1 and sprung mass m_2 in the neighbourhood of a equilibrium point are written as Eqs. (2.14) and (2.15):

$$m_1\ddot{z}_1 + b_2(\dot{z}_1 - \dot{z}_2) + b_1(\dot{z}_1 - \dot{w}) + k_2(z_1 - z_2) + k_1(z_1 - w) = -f_s \tag{2.14}$$

$$m_2\ddot{z}_2 + b_2(\dot{z}_2 - \dot{z}_1) + k_2(z_2 - z_1) = f_s\,. \tag{2.15}$$

On account of the available capacity of the laboratory facilities, the maximal mass to be mounted is taken to be $m_2 = 86$ kg. The unsprung mass is taken as small as possible: $m_1 = 11.5$ kg, comprising a light aluminium platform (for the purpose of assembly), guiding and fixing elements.

The ratio of unsprung to the sprung mass is roughly 0.13. Parameters of passive elements were chosen such that natural frequencies of damped vibrations should coincide with those of a real system – around 1.5 Hz and 11 Hz [2, 5, 8, 13, 17].

2.3. Phenomenological model of a open-loop system

Underlying the synthesis of a phenomenological model are the physical laws governing the kinematics of a suspension, and the equation of force and flow equilibrium in a hydraulic actuator.

The model of a full active suspension is expressed in the form of state and output equations. To derive the equation of state, recall Eqs. (2.11), (2.13)–(2.15).

State variables are expressed in the form of Eq. (2.16):

$$\begin{aligned} &x_1 = z_2, \quad x_2 = \dot{z}_2, \quad x_3 = z_2 - z_1, \quad x_5 = P_r = \frac{f_s}{A_a}, \quad x_6 = u_1\,, \\ &x_4 = \int\left[-\left(\frac{k_2}{m_2} + \frac{k_2}{m_1}\right)\cdot(z_2 - z_1) + \frac{k_1}{m_1}\cdot(z_1 - w) + \left(\frac{A_a}{m_2} + \frac{A_a}{m_1}\right)\cdot\frac{f_s}{A_a}\right]\mathrm{d}t\,. \end{aligned} \tag{2.16}$$

The first three variables of state are the displacement and velocity of the sprung mass and displacement of the sprung mass in relation to the unsprung mass. These parameters are measurable and adequately describe the system dynamics, hence they can be well used as feedback signals. State variable x_4 is derived after transformations of Eqs. (2.14), (2.15). This part is not utilised to derive other state variables. Variables x_5, x_6 describe the actuator dynamics,

representing the pressure difference in the chambers and spool displacement obtained from Eq. (2.13).

A nonlinear part Φ (Eq. (2.18)) is isolated from Eq. (2.11) such that matrices $\mathbf{A}$ and $\mathbf{B}$ in the state equations should contain linear terms only.

For thus defined variables, the state equations are written as:

$$\begin{bmatrix} \dot{x}_1 \\ \dot{x}_2 \\ \dot{x}_3 \\ \dot{x}_4 \\ \dot{x}_5 \\ \dot{x}_6 \end{bmatrix} = \mathbf{A} \cdot \begin{bmatrix} x_1 \\ x_2 \\ x_3 \\ x_4 \\ x_5 \\ x_6 \end{bmatrix} + \mathbf{B} \cdot \begin{bmatrix} v \\ w \end{bmatrix} + \mathbf{A}_\Phi \cdot \Phi, \qquad y = \mathbf{C} \cdot \begin{bmatrix} x_1 \\ x_2 \\ x_3 \\ x_4 \\ x_5 \\ x_6 \end{bmatrix} \tag{2.17}$$

where:

$$\mathbf{A} = \begin{bmatrix} 0 & 1 & 0 & 0 & 0 & 0 \\ -\dfrac{b_1 \cdot b_2}{m_1 \cdot m_2} & 0 & \dfrac{b_2}{m_2} \cdot \left(\dfrac{b_1}{m_1} + \dfrac{b_2}{m_1} + \dfrac{b_2}{m_2} \right) - \dfrac{k_2}{m_2} & -\dfrac{b_2}{m_2} & \dfrac{A_a}{m_2} & 0 \\ \dfrac{b_1}{m_1} & 0 & -\left(\dfrac{b_1}{m_1} + \dfrac{b_2}{m_1} + \dfrac{b_2}{m_2} \right) & 1 & 0 & 0 \\ \dfrac{k_1}{m_1} & 0 & -\left(\dfrac{k_1}{m_1} + \dfrac{k_2}{m_1} + \dfrac{k_2}{m_2} \right) & 0 & \dfrac{A_a}{m_1} + \dfrac{A_a}{m_2} & 0 \\ -A_a \alpha \dfrac{b_1}{m_1} & 0 & A_a \alpha \left(\dfrac{b_2}{m_2} + \dfrac{b_2}{m_1} + \dfrac{b_1}{m_1} \right) & -A_a \alpha & -C_{tm} \alpha & 0 \\ 0 & 0 & 0 & 0 & 0 & -\dfrac{1}{\tau} \end{bmatrix},$$

$$\mathbf{B} = \begin{bmatrix} 0 & 0 \\ 0 & \dfrac{b_1 \cdot b_2}{m_1 \cdot m_2} \\ 0 & -\dfrac{b_1}{m_1} \\ 0 & -\dfrac{k_1}{m_1} \\ 0 & A_a \alpha \dfrac{b_1}{m_1} \\ \dfrac{k_{sv}}{\tau} & 0 \end{bmatrix}, \quad \mathbf{C} = \begin{bmatrix} 1 & 0 & 0 & 0 & 0 & 0 \end{bmatrix}, \quad \mathbf{A}_\Phi = \begin{bmatrix} 0 & 0 & 0 & 0 & 1 & 0 \end{bmatrix}^T,$$

$$\Phi = \alpha l C_d x_6 \sqrt{\frac{P_z - \operatorname{sign}(x_6)\, x_5}{\rho}}\,. \tag{2.18}$$

Both v and w are inputs, yet the displacement w is treated as disturbance while v is the control voltage. Accordingly, the matrix $\mathbf{B}$ can be transformed:

$$\mathbf{B}_v = \mathbf{B} \cdot \begin{bmatrix} 1 \\ 0 \end{bmatrix}, \qquad \mathbf{B}_w = \mathbf{B} \cdot \begin{bmatrix} 0 \\ 1 \end{bmatrix}. \tag{2.19}$$

The equations of state will be rewritten as:

$$\begin{aligned} \dot{\mathbf{x}} &= \mathbf{A}\mathbf{x} + \mathbf{B}_v v + \mathbf{B}_w w + \mathbf{A}_\Phi \Phi, \\ y &= \mathbf{C}\mathbf{x}, \end{aligned} \tag{2.20}$$

where v and w are scalar quantities.

2.4. Linearising of the phenomenological model

The nonlinear model is approximated with the linear one in the neighbourhood of its working point. The method was applied whereby the nonlinear part of the equation of state 2.20 was expanded in the Taylor series. The working point is taken as the spool mid-position and the pressure difference (x_{6_0}, x_{5_0}) equal to zero, as in the static state the spool mid-position is associated with pressure equilibrium in the cylinder chambers. Thus the assumed working point does not cause the state variables to be shifted, since the value of the function at the working point is zero.

In the low frequency range of operation of the vibration control system (up to 20 Hz) and hence of the servovalve, an assumption is made that the negative value of the spool position x_6 corresponds to a negative pressure difference in the chambers, the positive value of the spool position is associated with the positive pressure difference. Assuming that the **sign** function is given as

$$\text{sign } x = \begin{cases} -1 & \text{for} \quad x < 0 \\ 0 & \text{for} \quad x = 0 \\ 1 & \text{for} \quad x > 0 \end{cases}$$

Equation (2.18) can be rewritten as

$$\Phi = \alpha l C_d x_6 \sqrt{\frac{P_z - |x_5|}{\rho}}. \tag{2.21}$$

It is readily apparent that the function Φ is continuous at the specified working point and can be thus linearised. Accordingly, Eq. (2.21) can be expressed as

$$\Delta\Phi = \left[\frac{\partial \Phi\,(x_5, x_6)}{\partial x_5}\right]_{x_{5_0}} \cdot \Delta x_5 + \left[\frac{\partial \Phi\,(x_5, x_6)}{\partial x6}\right]_{x_{6_0}} \cdot \Delta x_6\,. \tag{2.22}$$

The calculations were performed:

$$\left[\frac{\partial \Phi(x_5, x_6)}{\partial x_5}\right]_{x_{5_0}} = \left[-\frac{1}{2}\alpha l C_d x_6 \frac{1}{\sqrt{\dfrac{P_z - |x_5|}{\rho}}} \cdot \frac{\operatorname{sign}(x_5)}{\rho}\right]_{x_{5_0}} = 0,$$

$$\left[\frac{\partial \Phi(x_5, x_6)}{\partial x_6}\right]_{x_{6_0}} = \left[\alpha l C_d \sqrt{\frac{P_z - |x_5|}{\rho}}\right]_{x_{6_0}} = \alpha l C_d \sqrt{\frac{P_z}{\rho}}.$$

The continuity condition of the partial derivative of the function Φ at the working point was checked. Hence, substituting into Eq. (2.22) yields a linearised form of Eq. (2.18)

$$\Phi = \alpha l C_d \sqrt{P_z/\rho}\,(x_6 - x_{6_0}) = \alpha l C_d \sqrt{P_z/\rho}\, x_6\,. \tag{2.23}$$

Alternatively, a numerical procedure can be applied to linearise Eq. (2.18). Knowing the applicable range of the function of state variables x_5, x_6, one can generate input data vectors x_5, x_6 and an output vector Φ, basing on a nonlinear equation. The numerical data are then written as an equation of linear regression of two input variables, which allows the nonlinear function Φ to be approximated with a linear equation in the predetermined range of state variables. This problem was solved using the Matlab package. Regression coefficients were found, hence Eq. (2.18) can be replaced by function (2.24) that captures state variables in the interval $x_5 = \pm 7$ MPa and $x_6 = \pm 0.25$ mm:

$$\Phi = -341.2 \cdot x_5 + 4.666 \cdot 10^{13} \cdot x_6\,. \tag{2.24}$$

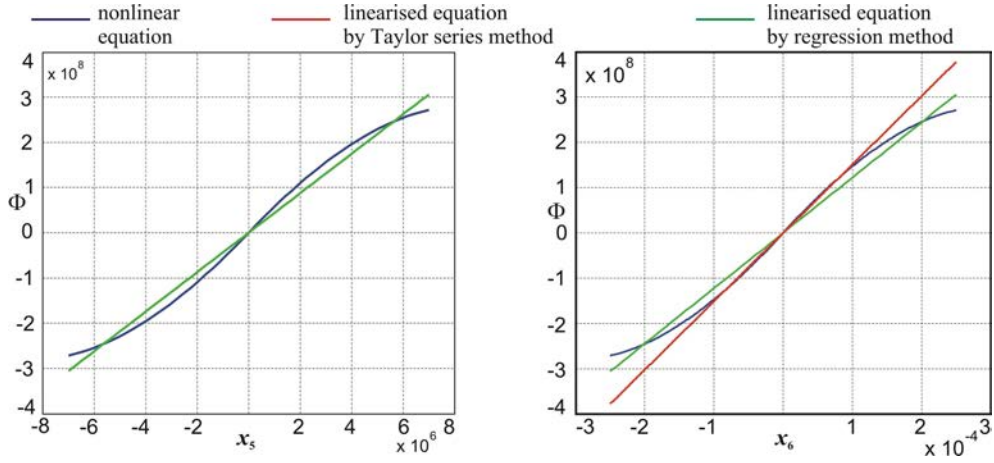

FIG. 4. Comparison of plots $\Phi(x_5)$ and $\Phi(x_6)$ obtained basing on nonlinear equation and equations linearised by the two methods.

Figure 4 shows representation of a nonlinear Eq. (2.18) by linearised Eqs. (2.23), (2.24). In order to establish how linearisation should affect the dynamic properties of the object's model, amplitude-frequency characteristics were obtained: $20\log_{10}(z_2/v)$ and $20\log_{10}(z_2/w)$ (Fig. 5).

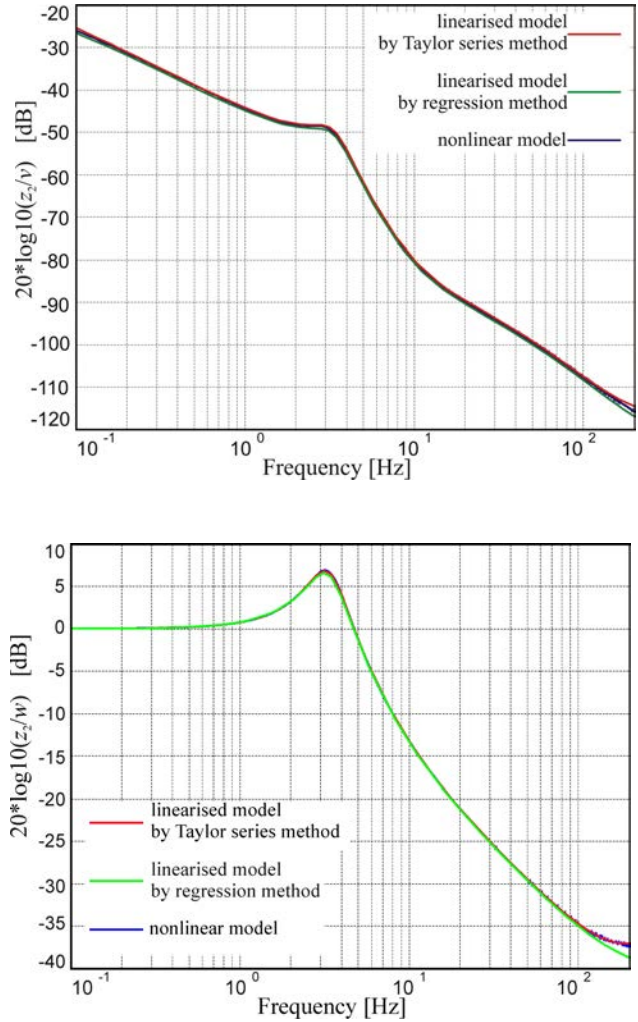

FIG. 5. Comparison of amplitude-frequency characteristics of sprung mass displacement relative to inputs to the nonlinear model and linearised model.

These confirm that representation of a nonlinear model by a linear one is correct throughout the whole investigated frequency range.

Underlying the mathematical model are relationships defining the properties of open-loop models, so the model can be expressed in a linear form. Synthesis

of this model allows for finding physical relationships describing the model of a structure. State variables were selected that well portray the dynamic properties of the investigated structure. Comparison of response times of the phenomenological model and that obtained in the procedure of identification against response times of a laboratory, the physical model enables us to verify the adequacy of identification procedure.

3. Identification of the parametric model

The identification method consists in finding the coefficients in the first-order differential equations governing the system dynamics. The multi-dimensional linear regression method is applied. During the laboratory tests the physical model of a parallel structure was subjected to random excitations, fed to both inputs. The registered parameters include: preset kinematic excitation w, preset control voltage to the servovalve v, outputs: displacement of the sprung mass z_2, displacement of the unsprung mass z_1, pressures in the cylinder chambers P_d, P_g, actuator supply pressure P_z, instantaneous flow rates Q_z between the supplying unit and actuator. The acquired registered signals were pre-processed, which involved re-scaling, trend removal and elimination of high-frequency components. Derivatives of the acquired signals were obtained, too.

Basing on the created phenomenological model and other models available in the literature on the subject [5–7, 17–20], the following physical variables are selected as state vectors that describe the investigated object: $x_1 = z_2$, $x_2 = \dot{z}_2$, $x_3 = z_1$, $x_4 = \dot{z}_1$, $x_5 = P_r = P_d - P_g$. The sixth variable of state is the derivative of work performed by the unit supplying the actuator $x_6 = P_z Q_z$. Hence, x_6 becomes the measure of power absorbed from the unit. Thus the defined variables form a matrix $\mathbf{X}$, containing measured time series of state variables and time series of control variables v, w. The vector of parameters is estimated using the least square method, given by Eq. (3.1)

$$\hat{\boldsymbol{\beta}} = \left(\mathbf{X}^T\mathbf{X}\right)^{-1}\mathbf{X}^T\dot{x}_n\,, \tag{3.1}$$

where $n = 1, 2, ..., 6$.

The procedure of identification of the parameters vector utilises a dedicated computer program developed in Matlab. The parametric model of a quarter-vehicle suspension obtained from identification is governed by the equations:

$$\begin{aligned} \dot{x} &= \mathbf{A}x + \mathbf{B}\begin{bmatrix} v \\ w \end{bmatrix}, \\ y &= \mathbf{C}x, \end{aligned} \tag{3.2}$$

where

$$\mathbf{A} = \begin{bmatrix} 0 & 1 & 0 & 0 & 0 & 0 \\ -231 & -46 & 23 & 40 & 2504 & -401800 \\ 0 & 0 & 0 & 1 & 0 & 0 \\ 305 & 50 & -1248 & -77 & -3493 & 596600 \\ 2 & -1 & -6 & 1 & -53 & 10220 \\ 0 & 0 & 0 & 0 & 0 & -1 \end{bmatrix}, \quad \mathbf{B} = \begin{bmatrix} 0 & 0 \\ 4442 & 212 \\ 0 & 0 \\ -6879 & 949 \\ 47 & 4 \\ 0 & 0 \end{bmatrix},$$

$$\mathbf{C} = \begin{bmatrix} 1 & 0 & 0 & 0 & 0 & 0 \end{bmatrix}.$$

3.1. Model verification in the laboratory setup

The mathematical model was verified in the laboratory setup. The duly implemented of the suspension was subjected to kinematic excitations of square wave-form. Sine signal of frequency linearly increasing in time from 0.063 to 40 Hz was fed to the other input (voltage driving the actuator servovalve). The transition from the initial to the final frequency lasted 40 s. Input signals of different amplitudes were applied in the experiments, both input and output signals (displacement of sprung mass) were acquired. Figure 6 shows the time histories collected for the amplitude of excitations ±10 mm, control voltage amplitude ±3 V and response times of the phenomenological model and that estimated for the predetermined displacement w and voltage v.

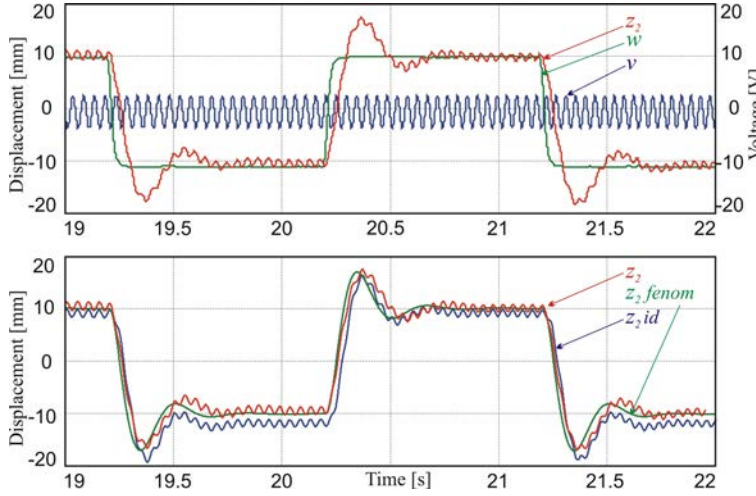

FIG. 6. Comparison of time responses of the: laboratory, phenomenological and estimated model for the set value of the displacement w and voltage v.

Both the phenomenological and estimated models well emulate the shape of the output signal from the object. The phenomenological model performance in

the high frequency range seems to be inferior. This model could be optimised through the tuning of parameters such as servovalve amplification gain, leakage between the chambers and geometric parameters of the spool. Since the model was used only to verify the estimated model and to find the process variables that control the object's dynamics, the test results are taken as satisfactory. The estimated model agrees better with the laboratory model and it takes into account the power consumed by the actuator. On account of above advantage, this model was selected for the synthesis of the control system.

Similar correspondence is obtained when simultaneous random excitations are applied on the inputs w, v. Utmost care must be taken to ensure that these signals should be non-correlated.

4. Dynamic properties of the open loop model

Dynamic properties of the open loop model of a full active structure can be determined on the basis of the model obtained from identification. Similarly to the synthesis of a phenomenological model, the control matrix $\mathbf{B}$ in the identified model has two components: $\mathbf{B}_v$, $\mathbf{B}_w$, corresponding to two inputs to the system: control input v and excitation w. Equation (3.2) can be rewritten as:

$$\begin{aligned} \dot{\mathbf{x}} &= \mathbf{A}\mathbf{x} + \mathbf{B}_v v + \mathbf{B}_w w, \\ y &= \mathbf{C}\mathbf{x}. \end{aligned} \tag{4.1}$$

Figure 7 shows a block diagram of quarter-vehicle suspension model associated with Eq. (4.1).

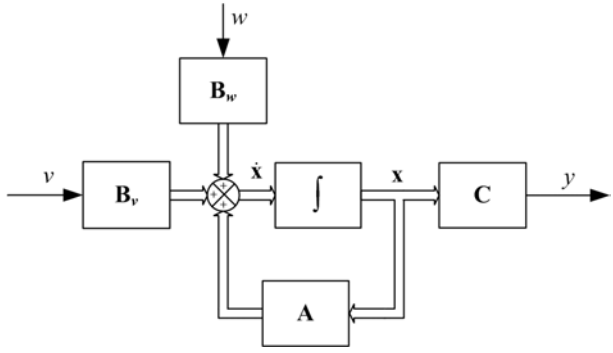

Fig. 7. Block diagram of the vehicle suspension model.

Characteristic equation for the matrix $\mathbf{A}$ is derived from the formula

$$\begin{aligned} &|s\mathbf{I} - \mathbf{A}| = 0\,, \\ &s^6 + 177s^5 + 15713s^4 + 300095s^3 + 6612388s^2 + 14887015s + 8559185 = 0\,. \end{aligned} \tag{4.2}$$

Solving Eq. (4.2) yields the eigenvalues of the matrix **A**:

$$\lambda_1 = -1, \qquad \lambda_2 = -1.439,$$
$$\lambda_3 = -7.495 + j20.570, \qquad \lambda_4 = -7.495 - j20.570,$$
$$\lambda_5 = -79.786 + j77.775, \qquad \lambda_6 = -79.786 - j77.775.$$

Eigenvalues placement on the complex plane is shown in Fig. 8.

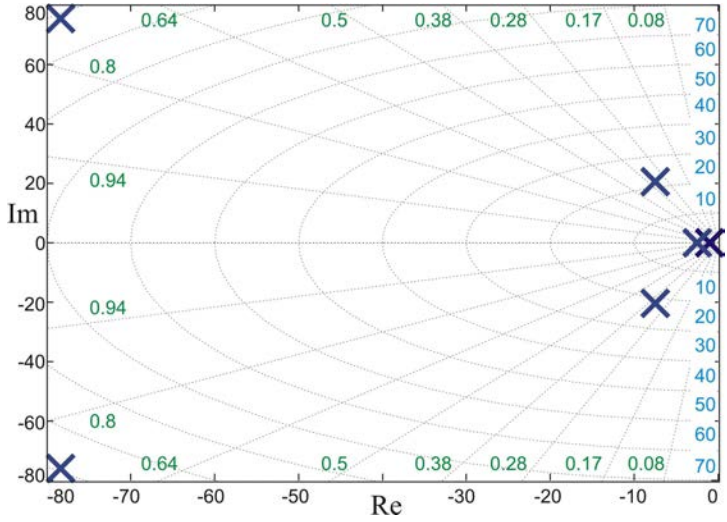

FIG. 8. Eigenvalues placement on the complex plane.

For each eigenvalue the natural frequency f_0 and the damping ratios coefficient ξ are derived from Eqs. (4.3) and (4.4):

$$f_{0i} = \frac{|\lambda_i|}{2\pi} = \frac{\sqrt{\mathrm{Re}^2(\lambda_i) + \mathrm{Im}^2(\lambda_i)}}{2\pi}, \tag{4.3}$$

$$\xi_i = \cos(\beta_i), \tag{4.4}$$

where β_i denotes the angle between the eigenvector and the real axis in the coordinate system. It is obtained from the formula $\beta_i = \mathrm{arctg}\left(\dfrac{\mathrm{Im}(\lambda_i)}{\mathrm{Re}(\lambda_i)}\right)$. Natural frequencies and damping ratios coefficients computed for the eigenvalues of the matrix **A** are:

$$f_{01} = 0.15915 \text{ Hz}, \qquad \xi_1 = 1,$$
$$f_{02} = 0.22894 \text{ Hz}, \qquad \xi_2 = 1,$$
$$f_{03} = f_{04} = 3.4843 \text{ Hz}, \qquad \xi_3 = \xi_4 = 0.34234,$$
$$f_{05} = f_{06} = 17.733 \text{ Hz}, \qquad \xi_5 = \xi_6 = 0.71607.$$

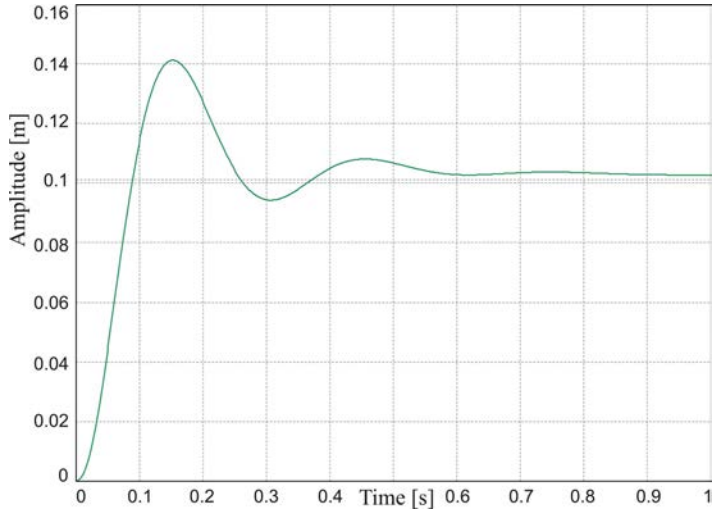

FIG. 9. Suspension step response (0.1 m) without controller.

Figure 9 shows the response of an open-loop system to a step of 0.1 m, Fig. 10 shows the amplitude-frequency characteristics in relation to the excitation w. This is an equivalent of the transfer function defined as the ratio of vibration amplitudes at the output $y = z_2$ to that at the input w, expressed in dB, for the frequency range 0.1–100 Hz.

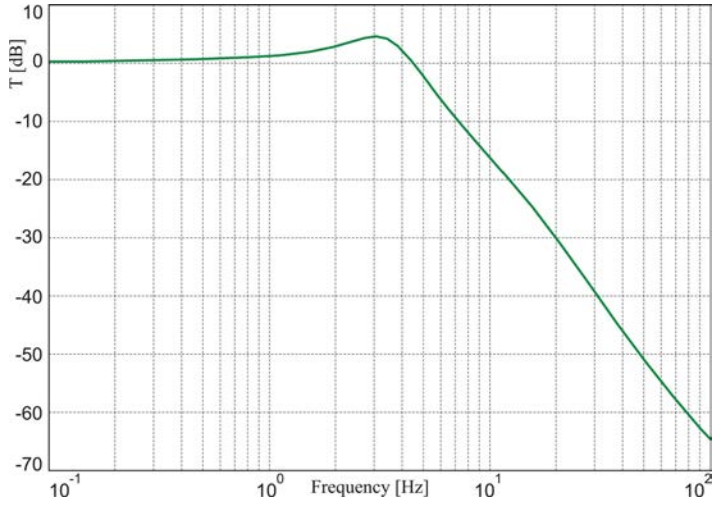

FIG. 10. Vibration displacement transmissibility in the function of frequency.

Characteristics (Figs. 9, 10) are based on the simulations of the identified model under the actuator control voltage equal to zero ($v = 0$). The designed

controller should reduce the vibration amplification in the neighbourhood of resonance frequency $f_0 = 3.4843$ Hz and reduce their displacement transmissibility in the whole frequency range.

From the standpoint of vibration control performance, the transmissibility characteristics is the key measure of quality of the vibration control system. The amplitude-frequency characteristic of the output z_2 in relation to the input v (servovalve control) agrees well with that obtained for the phenomenological model shown in Fig. 5.

5. Conclusions

Properties of actuators generating active force in vibration reduction systems in vehicles are neglected in most models used for the synthesis of control systems. These properties are often assumed to be those of a proportional element. However, taking them into account in a suspension model allows us to evaluate nonlinear features introduced by this very element. In the case of an electrohydraulic actuator, linearisation of the suspension model (in the effective range of state vector variations) does not bring about any major changes that would preclude its use. Both the phenomenological model and that obtained from identification correctly portray the static and dynamic properties of the investigated object. The estimated model agrees better with the laboratory model, furthermore it enables us to evaluate the power consumption by the actuator. The component of the state vector in this model is defined as the power absorbed by an actuator from the supply source. In this approach, power consumption by an actuator and vibration isolation performance can be determined already at the stage of design of the control system. It is a well-established fact that high energy consumption in active vibration control system is the key reason why these systems are rarely employed, so the model proposed by the author might be used in synthesis of a system with lower demands for external power.

References

1. J. Bajkowski, W. Grzesikiewicz, L. Orłowski, *Model matematyczny oraz badania eksperymentalne elementów zawieszenia szybkobieżnego pojazdu gąsienicowego*, Zeszyty Naukowe P.P., Wyd. Polit. Poznańska, **54**, 23–30, 2002.
2. D. A. Crolla, M. B. A. Abdel–Hady, *Active suspension control; performance comparisons using control laws applied to a full vehicle model*, Vehicle System Dynamics, **20**, 107–120 1991.
3. M. D. Donahue, *Implementation of an Active Suspension, Preview Controller for Improved Ride Comfort*, University of California – Berkeley 2001.
4. J. Grajnert, *Izolacja drgań w maszynach i pojazdach*, Wydawnictwo Politechniki Wrocławskiej – Wrocław 1997, ISSN 1425-0993.

5. C. H. Hansen, S. D. Snyder, *Active control of noise and vibration*, E & FN SPON: Chapman and Hall, London 1997.

6. D. Hrovat, *Survey of advanced suspension developments and related optimal control applications*, Automatica, **33**, 10, 1781–1817, 1997.

7. R. Johansson, A. Rantzer, *Nonlinear and Hybrid systems in automotive control*, Springer, 2003.

8. D. Karnopp, *Vehicle stability*, Marcel Dekker, New York 2004.

9. J. A. Levitt, N. G. Zorka, *Influence of tire damping in quarter car active suspension models*, Journal of Dynamic Systems, Measurement and Control: Transactions of the ASME, **113**, 134–137, 1991.

10. R. Palej, *Dynamika i stateczność aktywnych pneumatycznych układów wibroizolacji*, Seria Mechanika – Monografia 218 Wydawnictwo Politechniki Krakowskiej, Kraków 1997, PL ISSN 0860-097X.

11. A. Pizoń, *Hydrauliczne i elektrohydrauliczne układy sterowania i regulacji*, WNT, Warszawa 1987.

12. J. Pluta, J. Konieczny, R. Korzeniowski, *Badanie pneumatycznych układów redukcji drgań mechanicznych*, PNEUMA'2000: XII Krajowa Konferencja Pneuma' 2000 Kielce 2000, Wydawnictwo Politechniki Świętokrzystkiej – Zeszyty Naukowe Elektryka, **39**, 269–278, PL ISSN 0239-4960.

13. R. Rajamani, *Vehicle dynamics and control*, Springer, 2006.

14. Mannesmann Rexroth Catalogue.

15. J. T. Viersma, *Analysis, synthesis and design of hydraulics servosystems and pipelines*, Amsterdam, Elsevier Scientific Publishing Company, 1980.

16. G. R. Wendel, G. L. Stecklein, *A regenerative active suspension system. Vehicle Dynamics and Electronic Controlled Suspensions*, SAE Special Publication Number 861, 129–135, 1991.

17. S. Yildirim, *Vibration control of suspension using a proposed neural network*, Journal of Sound and Vibration, **277**, 1059–1069, 2004.

18. F. Yu, D. A. Crolla, *An optimal self-tuning controller for an active suspension*, Vehicle System Dynamics, **29**, 51–65, 1998.

19. F. Yu, D. A. Crolla, *State observer design for an adaptive vehicle suspension*, Vehicle System Dynamics, **30**, 457–471, 1998.

20. A. Zaremba, *Optimal active suspension design using constrained optimization*, Journal of Sound and Vibration, **207**, 3, 351–364, 1997.

Received July 19, 2007; revised version January 17, 2008.